Printing of Sub-100-nm Metal Nanodot Arrays by Carbon Nanopost Stamps

Sang Ho Lee,[†] Byungjin Cho,[†] Seungha Yoon,[†] Huisu Jeong,[†] Sangyong Jon,[‡] Gun Young Jung,[†] Beong Ki Cho,[†] Takhee Lee,[†] and Won Bae Kim[†,*]

[†]School of Materials Science and Engineering, Gwangju Institute of Science and Technology (GIST), Gwangju 500-712, Republic of Korea and [‡]School of Life Science, Gwangju Institute of Science and Technology (GIST), Gwangju 500-712, Republic of Korea

ABSTRACT This work reports an efficient method to fabricate hexagonally patterned metal nanodot arrays at the sub-100-nm scale, which is based on contact printing *via* novel nanometer-scaled stamps. Vertically aligned carbon nanoposts, supported by hexagonally ordered nanochannels of anodic aluminum oxide templates, are employed as the stamping platform to directly transfer controlled metal nanodot arrays. Using the fabrication platform, a number of patterned metal nanodot arrays made of Au, Cu, Ni, Ag, Pt, Al, and Ti can be contact-printed over large substrate areas in ambient conditions. The size, density, and interdistance of the printed nanodots are controllable with a tight correspondence to the mother stamp geometries, which can be precisely tuned by modifying the pore dimensions of the alumina matrixes. An advanced example of contact printing of metal nanoparticles is successfully demonstrated by the controlled formation of nanodot arrays in a specific area.

KEYWORDS: contact printing · sub-100-nm metal nanodots · carbon nanopost stamp · hexagonal arrangement · selective area patterning

Uniformly controlled metal nanodot arrays with sizes under 100 nm have attracted much attention for diverse applications in nanotechnology including photoelectrical devices,[1,2] magnetic data storage,[3,4] biological sensors,[5,6] and catalysts for one-dimensional nanostructure growth.[7,8] For practical implementation, the ability to prepare uniform and controlled metal nanodot arrays in an effective process is of considerable interest in nanofabrication. Until nzow, several approaches for forming regular metal dot arrays with sub-100-nm size have been proposed. For example, template-assisted methods offer excellent homogeneity in dot size and high throughput over a large area, but the handling and removal of ultrathin porous template sheets lead to inconvenience in the manufacturing processes.[9] Lithographic attempts using focused ion beams or electron beams (e-beam) can manipulate the location of metal nanodots and offer precise control of dot dimensions, but these methods, unfortunately, suffer from complicated and expensive fabrication procedures and low throughput.[10]

A contact printing method that uses a stamp with raised and recessed configurations can be an effective method of nanofabrication with the advantages of simplicity, low cost, and high throughput.[11] The printing process can manufacture small structures without expensive or complicated equipment by simply transferring various types of materials onto large-area substrates at one time. For successful nanofabrication using the printing method, high-quality stamps with nanometer-scale geometries are indispensable. Polydimethylsiloxane (PDMS) has most commonly been exploited as a stamp material by many lithographic research groups because of its flexibility, ascribed to its low Young's modulus (360−870 kPa), which permits intimate contact and repeated stamping.[12] Despite its fascinating nature, however, there still remains a strong desire for the development of more efficient stamping instruments that enable sub-100-nm size metal nanodots to be transferred in patterns. To prepare and control the topographical features of PDMS-based stamps, time-consuming and cost-competitive lithographic processes such as photolithography or e-beam lithography have been exploited.[13] Furthermore, there are size restrictions on the fabrication of PDMS materials as a nanopost architecture for printing sub-100-nm metal nanodots.[14]

In this paper, a novel fabrication platform for uniform, highly patterned, and sub-100-nm metal nanodot arrays *via* the contact printing method is reported. Hexagonally arranged carbon nanopost (CNP) arrays, chemically formed within porous channels of anodic aluminum oxide (AAO) matrixes, are employed as the stamp for printing controlled metal nanodot arrays. Using these printing platforms, a large number of different metal nanodots with sizes of 30−90 nm, such as Au, Cu, Ni, Ag, Pt, Al, and Ti, can be

* Address correspondence to wbkim@gist.ac.kr.

Received for review March 15, 2011 and accepted June 23, 2011.

Published online June 23, 2011
10.1021/nn2009722

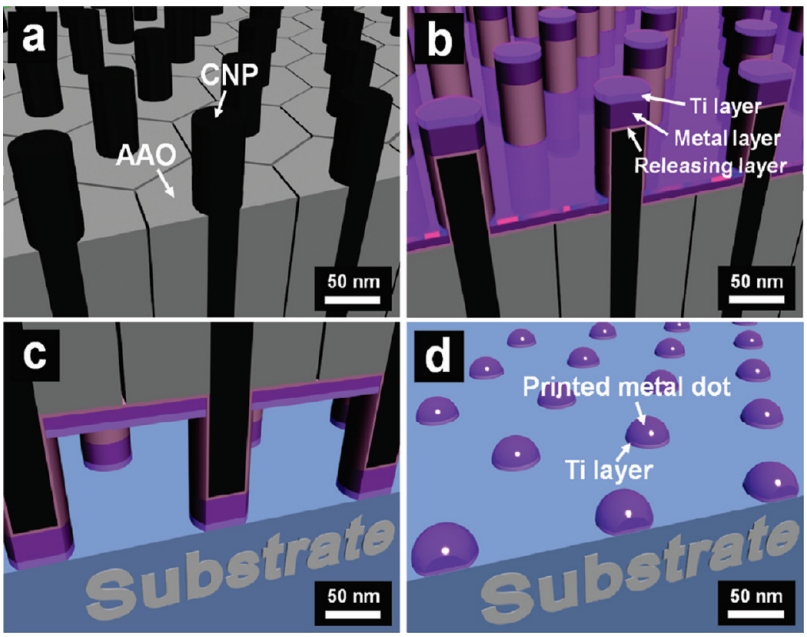

Figure 1. Schematic illustrations depicting the entire process, which includes (a) preparation of the CNP stamp, (b) loading of the metal layers on the pretreated CNP tips, (c) contact printing of the metal-loaded stamp onto the substrate, and (d) formation of controlled metal nanodot arrays.

explicitly printed over a large area in ambient laboratory conditions. The transferred metal nanodots are well aligned in the hexagonal pattern and show uniformity in their dimensions. The size, density, and interdot distance of the printed metal nanodots correspond precisely to the CNP stamp geometries, which can be systematically tuned by controlling the AAO pores. Furthermore, control of the location of metal nanodot arrays in specifically defined areas is successfully demonstrated, indicating that this contact printing system could be a powerful candidate to realize the large potential of the printing technique for sub-100-nm size nanodots with its simplicity, high throughput, versatility, reusability, and low cost for more practical applications such as photoelectronics and chemical sensing.

RESULTS AND DISCUSSION

The entire procedure used in this study is illustrated in Figure 1. The process consists of three stages: (i) fabrication of the CNP stamps, (ii) deposition of the metal layers on the CNP tips, and (iii) contact printing of the metal nanodot arrays on the substrate surface. The CNP stamps feature a composite configuration of vertical CNP arrays that are tightly held in the straight channels of nanoporous AAO templates (Figure 1a). As the AAO templates enable the CNPs to remain vertically aligned, the CNP arrays can bear the external pressure during contact printing. The diameter, density, and interval of the aligned CNPs can be modified along with the pore geometry of the AAO template. The next step is the deposition of metal layers onto the CNP tips, where surface treatment of the stamps is vital for successful metal nanodot transfer (see the illustration of the metal-deposited CNP stamp in Figure 1b). The metal transfer mechanism is based on the difference in adhesion strength between the stamp-metal and substrate-metal interfaces.[15] Therefore, the stamp surface should be properly modified; the surface adhesion of the metal to the substrate should be much larger than that to the stamp tips. In this experiment, to reduce cohesion between the CNP surface and the loaded metal layers, the stamp was chemically coated with a self-assembled monolayer (SAM) of tridecafluoro-1,1,2,2-tetrahydrooctyltrichlorosilane ($CF_3(CF_2)_5(CH_2)_2$-$SiCl_3$).[16,17] The Si−Cl terminal groups of the release agent strongly react with the hydroxyl (−OH) groups on the CNP surface that are formed by oxygen treatment of the pristine stamp surfaces, which can provide chemisorption sites for perfluoroalkyl trichlorosilane molecules. This reaction results in the Si−O−CNP chemical linkage at the interface between the release agent molecules and the stamp surfaces.[17] After loading the desired metals on the pretreated CNP tips, a thin Ti layer is subsequently deposited over the metal layers. Ti layers are frequently used to promote the cohesive strength between a metal and a substrate and, hence, enable the metal layer to be readily transferred to the substrate surface. Finally, the metal-loaded stamps are contact-printed onto a precleaned Si substrate in the laboratory at room temperature (Figure 1c). During the printing process, as the Ti layers are in direct contact with the substrate surface, they function as the "glue" between the surfaces of the metal and the substrate. The metal nanodot transfer process assisted by the Ti layer is based on a common

condensation reaction between the −OH groups formed on both surfaces of the Ti layer and the substrate. The Ti layer spontaneously forms surface oxide species under ambient conditions, which can be easily hydroxylated. When two surfaces of the Ti layer activated with −OH groups and the Si substrate covered with the native oxide are brought into contact, the condensation reaction takes place at the interface, and this reaction results in the chemical bonding of Ti−O−Si[10] (from here, we denote "Si substrate" instead of "Si/SiO_x substrate" for convenience sake, although tiny passivated SiO_x layers exist on the Si substrate). After lifting the CNP stamp from the substrate, the metal nanodot arrays are left behind on the substrate (Figure 1d). The printed metal nanodots correspond to the size, density, and intervals of the CNP arrays, reproducing the same pattern of pristine stamps.

Previous studies have demonstrated several applications using the vertically aligned CNPs in various nanotechnology fields including nanometer-scale master molds for nanoimprint lithography,[16] nanosyringes for cellular delivery systems,[18] and nanoarchitectured electrodes for Li-ion storage.[19] Furthermore, a novel usage of CNP arrays as a tool to control the diameter of semiconductor SnO_2 nanowires was recently reported.[20] This present research focuses on the formation of various metal nanodot arrays controlled under 100 nm in size by contact printing using a nanometer-resolution stamping platform, which has rarely been attempted in conventional printing routes. The contact printing technique using the CNP stamps gives rise to remarkable scientific advantages. (1) Contact printing of sub-100-nm size nanodot arrays using the CNP arrays can be an extension of standard printing methodology because conventional stamping platforms have size restrictions for the printing of ordered nanodots less than 100 nm in size. (2) The fabrication of controllable metal nanodots by printing of the reusable stamp provides a simple, low-cost, and high-throughput nature. (3) Numerous metal nanodots, regardless of the nature of the metal, can be easily fabricated by using this platform. (4) The size, density, and interval of the printed nanodot arrays can be systematically controlled.

Figure 2a,b shows representative scanning electron microscopy (SEM) images of the CNP stamps used here. Vertically aligned CNP arrays were prepared by depositing pyrolytic carbons in the honeycomb-like nanochannels of AAO matrixes *via* thermal chemical vapor deposition (CVD), followed by mechanical and chemical etching treatments (see the Experimental Section for details). Flat and round-shaped CNP tips were arranged in hexagonally ordered patterns and separated by a constant interval, indicating that CNP stamps can act as an elegant platform for use in transferring uniform metal nanodot arrays. The CNPs exhibit a uniform size distribution of 50 ± 6 nm, which was precisely controlled in the straight nanochannels of the AAO templates.[20] A cross-sectional view (Figure 2b) distinctly reveals the configuration of the stamp, in which the CNPs are firmly sustained by the AAO templates, showing a constant height (*ca.* 60 nm) from the AAO surface. This uniformity in height combined with the flexibility of one-dimensional carbon structures[21,22] can bear the force applied perpendicular to the CNP tips, which enables the stamps to be reused after repeated stamping processes (see Figure S1 of the Supporting Information). Figure 2c,d presents SEM images of the metal-layer-loaded CNP stamps. Au metal layers were preliminarily deposited on the CNP tips, which were precoated with antisticking monolayers, and then adhesion-enhanced Ti layers (<2 nm in thickness) were loaded on the Au layers by e-beam evaporation. The tip size of the metal-loaded stamp exhibited a slight increase of *ca.* 10% (55 ± 8 nm) as compared with that of the pristine stamp, which should be ascribed to the metal deposition. From the cross-sectional SEM image (Figure 2d), it can be confirmed that metal loading was achieved on the vertically aligned and physically isolated CNPs without disturbing the original configuration of the CNP stamp. Moreover, the deposition of the metal layers appeared to occur more preferentially on the CNP tips because these regions might have a higher probability of receiving the evaporated metal atom flux.[19] For successful printing of uniform metal nanodot arrays, one of the most important factors is the exposed height (H_{exp}) of the CNPs from the AAO surface, which was predictably controlled by tuning the etching time.[16,18] For example, insufficiently tall CNP arrays (H_{exp} < 10 nm) do not seem to function properly, resulting in an agglomerated film-like structure after printing (see Figure S2 of the Supporting Information). In contrast, too tall CNPs (H_{exp} > 200 nm) are likely to aggregate into bundles because of the high aspect ratio,[16] which is again improper for use as a stamp. In this research, the CNP height was adjusted in the range 50 to 70 nm, which led to a good contact printing result. Figure 2e shows a SEM image of printed Au nanodot arrays on a Si substrate using the CNP stamps. The printed Au nanodots show excellent pattern isolation without aggregation. The size of the printed metal nanodots appears to be 58 ± 7 nm, indicating a slight increase as compared with the CNP tip diameter. The height of the printed nanodots shows a correlation to the thickness of the metal layers loaded on the CNP tips. The contact-printed nanodot arrays show quite robust adhesion strength. Even after the substrate with printed Au nanodot arrays was sonicated in an ethanol solvent for 30 min, no destruction or detachment of the printed nanodots was observed. Figure 2f presents the X-ray diffraction (XRD) spectra of (i) the printed Au nanodot arrays on the Si substrate, (ii) the Au-loaded CNP stamps, and (iii) the pristine CNP stamps,

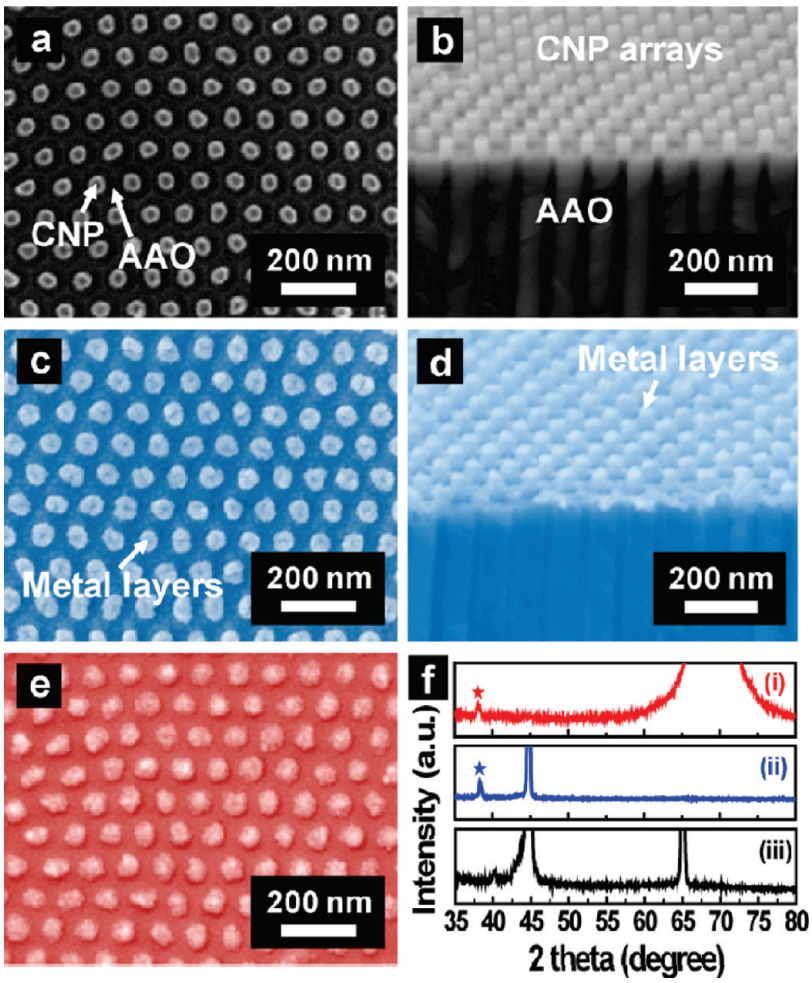

Figure 2. SEM images of the pristine CNP stamp with an average tip diameter of 50 nm ((a) top view and (b) cross-sectional view), the Au metal-layer-loaded stamp ((c) top view and (d) cross-sectional view), and (e) the Au nanodot arrays 58 nm in size contact-printed on a Si substrate. (f) XRD spectra indicating that the Au nanodots were explicitly transferred from the CNP tips to the Si substrate surface. The asterisk represents the crystallographic structure of Au(111).

which verifies the transfer of Au nanodot arrays from the CNP tips to the Si substrate. As a reference, the XRD spectrum for the CNP stamp itself reveals two different peaks from the CNP arrays and the AAO templates at $2\theta = 44.4°$ and 65.1°, respectively. In the XRD patterns of the Au metal-loaded CNP stamps before printing (Figure 2f(ii)), the peaks of Au(111) and carbon(100) from the CNP arrays can be distinctly observed at 38.2° and 44.4°, respectively, and the peak from the template is completely lost because of the deposition of metal layers. After contact printing of the Au-loaded stamp on the Si substrate (Figure 2f(i)), the diffraction spectra of the Au nanodots and Si substrate were only detected at 38.2° and 68.9°, respectively. The asterisk indicates the peaks of Au(111). Through the SEM and XRD inspections over the entire printed samples, no fraction of CNPs, which would be transferred to the substrate, has been observed. In addition to the Si substrate, the metal nanodot arrays were printed on various substrates, such as sapphire substrate, aluminum foil, and indium tin oxide glass (Figure S3 of the Supporting Information).

The size of the CNPs is readily controllable in the sub-100-nm range by tuning the pore dimensions of the AAO template, which represents one of the strengths of this work. The diameter of the AAO pores can be chemically adjusted by changing the nature of the electrolyte used and/or by pore expansion.[20,23] Figure 3a–c shows three stamps with different CNP sizes. A small-sized CNP stamp of 33 nm (Figure 3a) was fabricated in an AAO template that self-ordered in a sulfuric acid electrolyte. Stamps of 63 and 79 nm in size, as shown in Figure 3b,c, were synthesized in AAO matrixes produced from an oxalic acid electrolyte, followed by further pore-widening treatment in a chemical etching solution (see the Experimental Section). Consequently, four differently sized CNP stamps (*e.g.*, 33, 63, and 79 nm from Figure 3 and 50 nm from Figure 2) were demonstrated in this research. The packing density of the CNP arrays can also be modified according to the pore density of the template. The CNP stamp formed in the AAO matrix that self-organized in the sulfuric acid (Figure 3a) displays a much higher pore density (*ca.* 3×10^{10} cm^{-2})

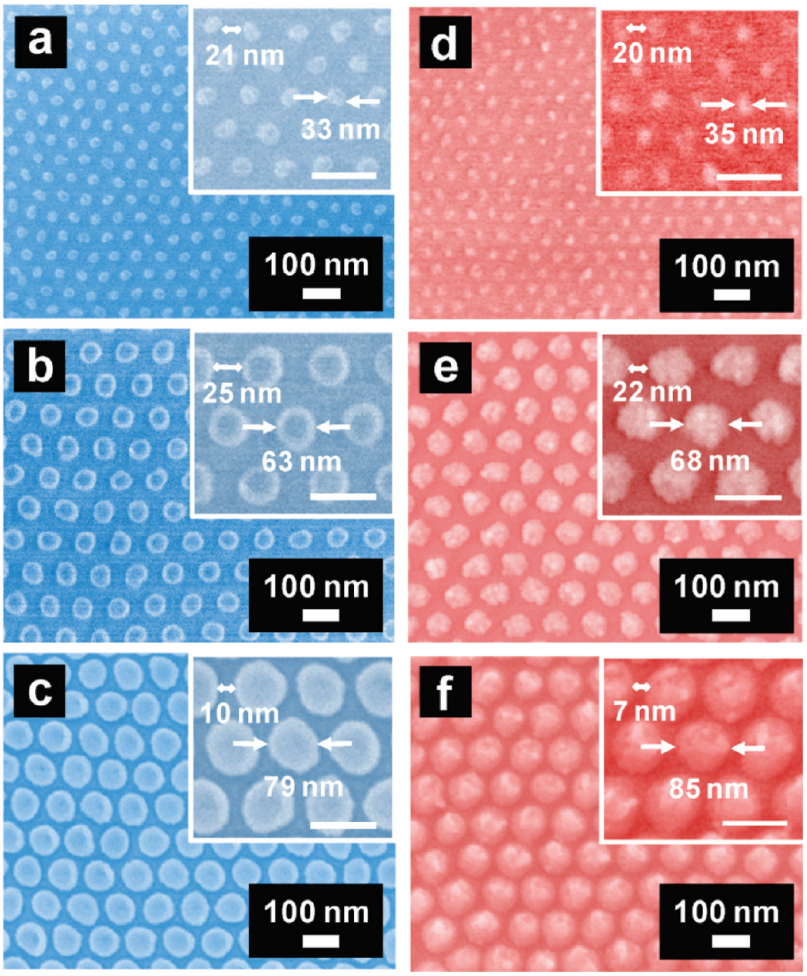

Figure 3. Typical SEM images of the CNP stamps with controlled tip sizes of (a) *ca.* 33 nm, (b) *ca.* 63 nm, and (c) *ca.* 79 nm. The printed Au nanodots show an average size of (d) 35 nm, (e) 68 nm, and (g) 85 nm. The magnified SEM images of the upper insets show the tight correspondence of the size, density, and interval between the CNP arrays and the contact-printed nanodot patterns.

than the stamps produced in the templates prepared in the oxalic acid (Figure 3b,c), in which the latter shows a pore density of *ca.* 1×10^{10} cm^{-2}. The interval between the CNPs can also be tuned by adjusting the size of the AAO pores. As the average CNP tip diameter is increased from 63 to 79 nm (Figures 3b,c), the interpost distance becomes smaller, and the interval is modified from 25 to 10 nm, respectively. For contact printing, the deposition of Au metal layers and Ti layers on the tips of three different CNP stamps was controlled under the same conditions, and the metal deposition was not affected by the morphology of the CNP stamps (see Figure S4 of the Supporting Information). Figure 3d–f presents SEM images of Au nanodot arrays printed on Si substrates by using these size-tuned CNP stamps. The printed metal nanodots display average sizes of 35, 68, and 85 nm, respectively, showing a tight size correspondence in accordance with the CNP diameter. In the smallest printed nanodots (Figure 3d), there exists some irregularity in the pattern accuracy. We speculate that the result might be attributed to the flexibility of the thin CNPs with an average diameter of 33 nm. As the geometries of CNP arrays can be systematically modified, the density and interdot distance of the printed Au nanodots can also be modulated. High-magnification images in each upper inset present an excellent correlation between the CNP stamps and the printed nanodot arrays, indicating that the contact printing technique using our tunable CNP arrays could be a compelling strategy to form controlled sub-100-nm metal nanodots.

Gold nanoparticles have been extensively used in the field of nanotechnology as plasmonic materials for the improved performance of optical devices,[24] catalysts for the synthesis of one-dimensional nanostructures,[25] and sensor electrodes for biochemical detection.[26] Given these applications, gold was selected as a standard material for printing using the CNP stamps in this work. In addition to gold, there are many other metal nanoparticles for applications in nanoscience and nanotechnology that would be useful if they were patterned on substrates with a nanometer-scale size less than 100 nm. Copper nanoparticles show potential applications for surface-enhanced Raman

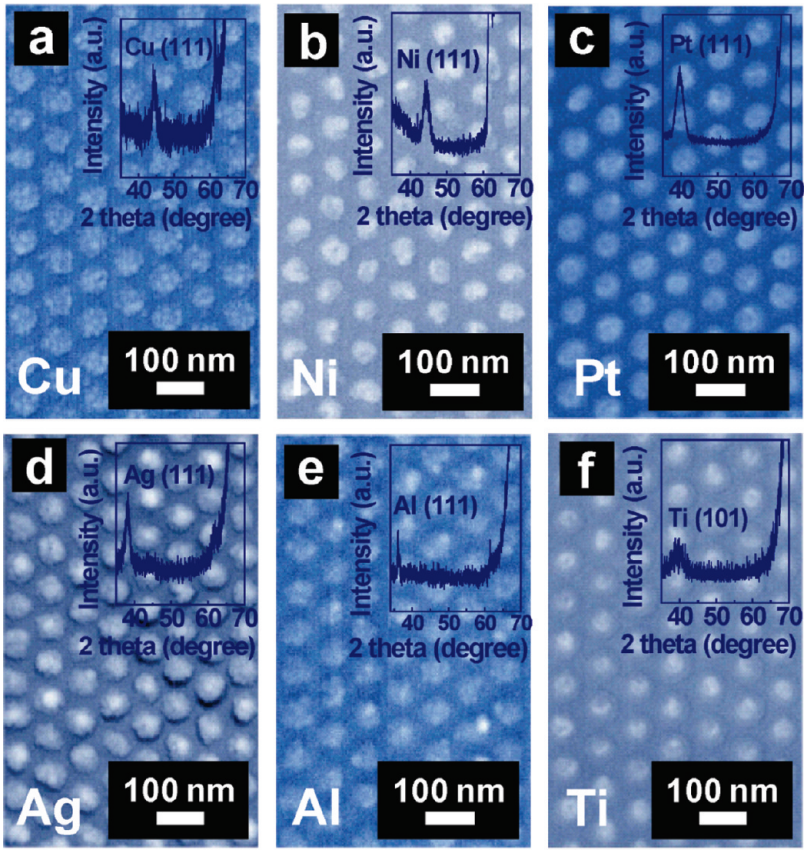

Figure 4. SEM images of various metal nanodot arrays printed by the CNP stamp with an average tip size of 63 nm: (a) Cu, (b) Ni, (c) Pt, (d) Ag, (e) Al, and (f) Ti. The XRD patterns in the insets show that the metal layers were explicitly transferred from the CNP stamps to the Si substrate (the strong peak at $2\theta = 68.9°$ in all of the XRD data indicates the lattice of a typical Si substrate). The various transfer results indicate that the contact printing method using CNP arrays can be an excellent platform for the fabrication of metal nanodot arrays.

spectroscopy;[27] nickel nanoparticles are important in ferromagnetic materials;[28] silver nanoparticles are attractive because they have excellent electrical and thermal conductivity;[29] platinum nanoparticles are commonly used as electrocatalysts in fuel cell devices;[30] aluminum nanoparticles are expected to be applied to next-generation propellants in the aerospace industry;[31] and titanium nanoparticles are expected to be promising for application in charge storage nodes for floating gate devices.[32]

Using this printing platform, it is most important to demonstrate that a wide range of metal nanodot arrays with sub-100-nm size can be printed in parallel, indicating the universality of this printing platform in the metal transfer system. The SEM images in Figure 4a–f show the printing results of various metal nanodot arrays made of Cu, Ni, Pt, Ag, Al, and Ti, respectively (the size distributions of the printed metal nanodots are provided in Figure S5 of the Supporting Information). The kinds of metal that can be used are not limited to the materials tested here. The metal layer deposition and contact printing process are almost the same as in the case of Au nanodot transfer. Each printed metal nanodot array is uniformly isolated in a hexagonal pattern and exhibits homogeneity in size consistent with the CNP diameter. The phases of transferred metal nanodot arrays were confirmed by XRD analysis, as included in the insets of Figure 4. In the XRD data, no additional diffraction peaks, excluding crystalline patterns from the printed metal nanodots and Si substrate, were detected. This contact printing technique should be applicable to the formation of any metal nanoparticles, which is difficult to achieve using other methodologies.

Technology that can selectively position metal nanodot arrays on desired places can play a key role in the assembly and design of nanodot-incorporated devices. Figure 5a shows a schematic illustration of selective area patterning of metal nanodot arrays. First, line-patterned shadow masks are placed on the top of CNP stamps (Figure 5a(ii)). Before setting the masks, the stamp surfaces are treated with a SAM coating with the releasing agent used before. Next the deposition of metal layers is carried out on the exposed region of the stamps by using e-beam evaporation, where the patterned shadow masks selectively screen the evaporated metal flux (Figure 5a(iii)). After removal of the shadow masks, the metal layers are exclusively loaded on the tips of CNP stamps that are disclosed to the evaporated flux (Figure 5a(iv)). Metal-loaded stamps

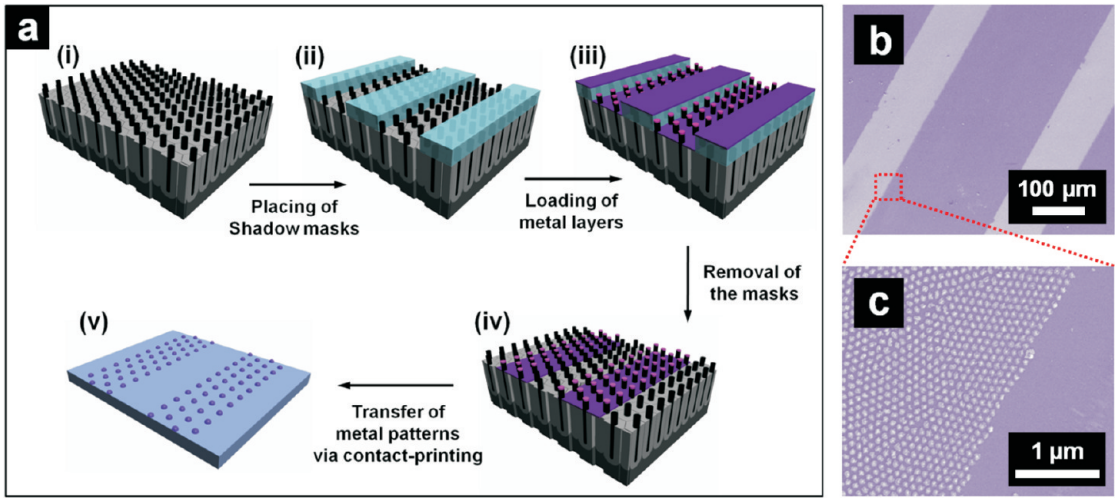

Figure 5. (a) Schematic diagram of selective patterning of metal nanodot arrays at exclusive sites: (i) fabrication of CNP stamps, (ii) placing of shadow masks, (iii) loading of metal layers on the exposed areas of the stamps, (iv) removal of the shadow masks and contact printing, and (v) selectively printed metal nanodot arrays. (b) Low-magnification SEM image of parallel line patterns (the lighter sites) produced by contact printing of selectively Au-loaded CNP stamps *via* shadow masks. (c) High-magnification SEM image of the printed line pattern edge, indicating that the Au nanodots are formed in selective areas. No Au nanodots are observed in the darker sites.

are then contact-printed on the surface of the substrate. The parallel line patterns consisting of metal nanodot arrays are transferred on the substrate (Figure 5a(v)). Figure 5b shows representative SEM images of the parallel line patterns that are printed on Si substrates by selectively Au metal-loaded CNP stamps. The parallel lines in the lighter region that were patterned with Au nanodots present a line width of *ca.* 100 μm and a spacing of *ca.* 220 μm, indicating that the printed results are strictly confined by the metal-loaded regions, as compared with the darker region in which no Au nanodots were observed. Figure 5c displays a high-magnification image, in which transferred Au nanodot arrays with an average size of *ca.* 68 nm are observed. (There is some irregularity on the nanodot patterns printed over a large scale. Formation of intrinsic grain boundary in the homemade AAO templates might be responsible for the irregularity of the pattern arrays, but this issue could be overcome by long-range ordering of the AAO template via the indentation process.[33]) Control of the location of metal nanodot arrays at desired sites could establish the basis of a potential application for the direct assembly of nanodot devices, especially for photoelectronics and sensor manufacturing, which is under investigation for the fundamental study of the surface plasmon resonance effect with the printed metal nanodot arrays.

CONCLUSION

In summary, an effective approach was developed to produce sub-100-nm metal nanodot arrays engineered by the contact printing method using novel nanostamping materials. Carbon nanopost arrays employed as nanostamps were fabricated using simple processes, and their size, interval, and density can be readily tuned. Using these nanostamps, hexagonally patterned metal nanodots of Au, Cu, Ni, Ag, Pt, Al, and Ti with controllable size, interval, and density were explicitly replicated by the printing process, which showed an excellent fidelity to the geometry of the pristine stamps. The controlled location of metal nanodot arrays in desired sites was explicitly embodied by contact printing of selectively metal-loaded stamps *via* line-patterned shadow masks. The capability to produce and control sub-100-nm metal nanodot arrays in an efficient method could play a key role in understanding the fundamental nature of nanoparticles and realizing potential applications in nanodot devices.

EXPERIMENTAL SECTION

Preparation of CNP Stamps. CNP stamps with controllable tip sizes were prepared by replicating AAO templates produced through a two-step anodization process under controlled conditions, as described elsewhere.[20,34] High-purity (99.999%) Al foils were degreased with acetone in an ultrasonic bath and then electrochemically polished in a mixture solution of $HClO_4$ and C_2H_5OH (1:5, v/v) at 5 °C under 15 V for 5 min. The pretreated Al sheets were anodized in a 0.3 M H_2SO_4 solution at 1 °C under 25 V, which formed an AAO template with a pore diameter of *ca.* 33 nm, or anodized in a 0.3 M $H_2C_2O_4$ solution at 13 °C under 40 V for a template with a pore size of *ca.* 50 nm. To obtain large-pore AAO templates, further pore-widening was performed over the AAO template with a 50-nm pore size by chemical wet etching in a mixture solution of H_3PO_4, CrO_3, and DI water (6:1.8:92.2 wt %) at 60 °C. The pore-opening processes were used to prepare AAO templates with pore sizes of *ca.* 63 nm and *ca.* 79 nm. Next, carbon layers were deposited on the

straight channel surfaces of the prepared AAO matrixes by using a thermal CVD method at 600 °C in a conventional tube furnace system without metallic catalysts. The AAO samples for carbon growth were placed in a tubular furnace, and then the temperature was elevated up to the reaction point (at a ramping rate of 20 °C min^{-1}) in an Ar atmosphere. Subsequently, the Ar gas was switched to a gas mixture of C_2H_2 and NH_3 at a rate of 20 and 80 sccm (standard cubic centimeter per minute); the carburization reaction proceeded for 4 h. After the carbon deposition, the furnace was cooled to room temperature. Finally, through selective exposure *via* dry etching using Ar ion milling followed by chemical wet etching in the etching solution, the vertically aligned CNPs remained on the surface. The exposed heights of the CNP arrays can be predictably controlled by manipulating the etching time as reported previously.[16,18]

Contact Printing Process Using CNP Stamps. The surfaces of the CNP stamps were treated with a SAM with $CF_3(CF_2)_5(CH_2)_2SiCl_3$ (tridecafluoro-1,1,2,2-tetrahydrooctyltrichlorosilane),[16,17] which served as the releasing layer between the CNP tips and the loaded metal layers. Before coating the release agent, the surfaces of the CNP stamp were treated with oxygen plasma by a UV-ozone generator for 10 min, which formed the −OH terminal groups on the CNP surfaces. Formation of SAMs on the stamp surfaces was conducted by the vapor-phase process at 10^{-2} Torr with two cycles.[17] After the coating process, the sample was rinsed with hydrofluoroether solvent. The desired metal layer (4 nm in thickness) was then deposited on the tips of the surface-pretreated CNP stamps, and a thin adhesion Ti layer (2 nm in thickness) was loaded on the top of the metal by an e-beam evaporator. In this experiment, the deposition condition of the metal layers on the CNP tips was almost the same regardless of the metals. The metal-loaded CNP stamps were directly printed onto precleaned Si substrates in an ambient environment under controlled pressure (0.1 MPa) for short contact times (less than 5 s) without heating. Both the stamp and substrate were fixed by a holder during the contact printing.

Acknowledgment. This work was supported by the National Research Foundation of Korea (NRF) grant funded by the Korean government (MEST) (No. R15-2008-006-03002-0 and No. 20110016600) and by the GSR_IC Project through a grant provided by GIST in 2011.

Supporting Information Available: Reusability of the CNP stamps, the effect of the exposed height of CNP arrays on the contact printing process, printing of metal nanodot arrays on various substrates, deposition of the Au metal layers and Ti layers on the three different CNP stamps, and the size distribution of the printed nanodots. This material is available free of charge *via* the Internet at http://pubs.acs.org.

REFERENCES AND NOTES

1. Kim, S.-S.; Na, S.-I.; Jo, J.; Kim, D.-Y.; Nah, Y.-C. Plasmon Enhanced Performance of Organic Solar Cells Using Electrodeposited Ag Nanoparticles. *Appl. Phys. Lett.* **2008**, *93*, 073307.
2. Lee, J. H.; Park, J. H.; Kim, J. S.; Lee, D. Y.; Cho, K. High Efficiency Polymer Solar Cells with Wet Deposited Plasmon Gold Nanodots. *Org. Electron.* **2009**, *10*, 416–420.
3. Natali, M.; Lebib, A.; Cambril, E.; Chen, Y.; Prejbeanu, I. L.; Ounadjela, K. Nanoimprint Lithography of High-Density Cobalt Dot Patterns for Fine Tuning of Dipole Interactions. *J. Vac. Sci. Technol. B* **2001**, *19*, 2779–2783.
4. Moritz, J.; Dieny, B.; Nozieres, J. P.; Landis, S.; Lebib, A.; Chen, Y. Domain Structure in Magnetic Dots Prepared by Nanodimprint and E-Beam Lithography. *J. Appl. Phys.* **2002**, *91*, 7314–7316.
5. Stadler, B.; Solak, H. H.; Frerker, S.; Bonroy, K.; Frederix, F.; Voros, J.; Grandin, H. M. Nanopattering of Gold Colloids for Label-Free Biosensing. *Nanotechnology* **2007**, *18*, 155306.
6. Zhang, Y.; Zeng, G.-M.; Tang, L.; Huang, D.-L.; Jiang, X.-Y.; Chen, Y.-N. A Hydroquinone Biosensor Using Modified Core-Shell Magnetic Nanoparticles Supported on Carbon Paste Electrode. *Biosens. Bioelectron.* **2007**, *22*, 2121–2126.
7. Papadopoulos, C.; Omrane, B. Nanometer-Scale Catalyst Patterning for Controlled Growth of Individual Single-Walled Carbon Nanotubes. *Adv. Mater.* **2008**, *20*, 1344–1347.
8. Lombardi, I.; Hochbaum, A. I.; Yang, P.; Carraro, C.; Maboudian, R. Synthesis of High Density, Size-Controlled Si Nanowire Arrays via Porous Anodic Alumina Mask. *Chem. Mater.* **2006**, *18*, 988–991.
9. Wang, S.; Yu, G. J.; Gong, J. L.; Zhu, D. Z.; Xia, H. H. Large-Area Uniform Nanodot Arrays Embedded in Porous Anodic Alumina. *Nanotechnology* **2007**, *18*, 015303.
10. Loo, Y.-L.; Willett, R. L.; Baldwin, K. W.; Rogers, J. A. Additive, Nanoscale Patterning of Metal Films with a Stamp and a Surface Chemistry Mediated Transfer Process: Application in Plastic Electronics. *Appl. Phys. Lett.* **2002**, *81*, 562–564.
11. Xia, Y.; Whitesides, G. M. Soft Lithography. *Angew. Chem., Int. Ed.* **1998**, *37*, 550–575.
12. Rolland, J. P.; Hagberg, E. C.; Denison, G. M.; Carter, K. R.; De Simone, J. M. High-Resolution Soft Lithography: Enabling Materials for Nanotechnologies. *Angew. Chem., Int. Ed.* **2004**, *43*, 5796–5799.
13. Kim, J.; Takama, N.; Kim, B. Reprint of "Fabrication of Nano-Structures Using Inverse-μCp Technique with a Flat PDMS Stamp. *Sens. Actuators A* **2007**, *139*, 356–363.
14. Rogers, J. A.; Nuzzo, R. G. Recent Progress in Soft Lithography. *Mater. Today* **2005**, *8*, 50–56.
15. Hur, S.-H.; Khang, D. -Y.; Kocabas, C.; Rogers, J. A. Nanotransfer Printing by Use of Noncovalent Surface Forces: Applications to Thin-Film Transistors That Use Single-Walled Carbon Nanotube Networks and Semiconducting Polymers. *Appl. Phys. Lett.* **2004**, *85*, 5730–5732.
16. Kim, Y.-S.; Lee, K.; Lee, J. S.; Jung, G. Y.; Kim, W. B. Nanoimprint Lithography Patterns with a Vertically Aligned Nanoscale Tubular Carbon Structure. *Nanotechnology* **2008**, *19*, 365305.
17. Jung, G.-Y.; Li, Z.; Wu, W.; Chen, Y.; Olynick, D. L.; Wang, S.-Y.; Tong, W. M.; Williams, R. S. Vapor-Phase Self-Assembled Monolayer for Improved Mold Release in Nanoimprint Lithography. *Langmuir* **2005**, *21*, 1158–1161.
18. Park, S.; Kim, Y. -S.; Kim, W. B.; Jon, S. Carbon Nanosyringe Array as a Platform for Intracellular Delivery. *Nano Lett.* **2009**, *9*, 1325–1329.
19. Kim, Y.-S.; Ahn, H.-J.; Nam, S. H.; Lee, S. H.; Shim, H.-S.; Kim, W. B. Honeycomb Pattern Array of Vertically Standing Core-Shell Nanorods: Its Application to Li Energy Electrodes. *Appl. Phys. Lett.* **2008**, *93*, 103104.
20. Lee, S. H.; Jo, G.; Park, W.; Lee, S. K.; Kim, Y.-S.; Cho, B. K.; Lee, T.; Kim, W. B. Diameter-Engineered SnO_2 Nanowires over Contact-Printed Gold Nanodots Using Size-Controlled Carbon Nanopost Array Stamps. *ACS Nano* **2010**, *4*, 1829–1836.
21. Poncharal, P.; Wang, Z. L.; Ugarte, D.; de Heer, W. A. Electrostatic Deflections and Electromechanical Resonances of Carbon Nanotubes. *Science* **1999**, *283*, 1513–1516.
22. Jaroenapibal, P.; Luzzi, D. E.; Evoy, S.; Arepalli, S. Transmission-Electron-Microscopic Studies of Mechanical Properties of Single-Walled Carbon Nanotube Bundles. *Appl. Phys. Lett.* **2004**, *85*, 4328–4330.
23. Masuda, H.; Asoh, H.; Watanabe, M.; Nishio, K.; Nakao, M.; Tamamura, T. Square and Triangular Nanohole Array Architectures in Anodic Alumina. *Adv. Mater.* **2001**, *13*, 189–192.
24. Morfa, A. J.; Rowlen, K. L.; Reilly, T. H., III; Romero, M. J.; van de Lagemaat, J. Plasmon-enhanced Solar Energy Conversion in Organic Bulk Heterojunction Photovoltaics. *Appl. Phys. Lett.* **2008**, *92*, 013504.
25. Comini, E.; Sberveglieri, G. Metal Oxide Nanowires as Chemical Sensors. *Mater. Today* **2010**, *13*, 36–44.
26. Fritzsche, W.; Taton, T. A. Metal Nanoparticles as Labels for Heterogeneous, Chip-Based DNA Dectection. *Nanotechnology* **2003**, *14*, R63–73.
27. Wang, Y.; Asefa, T. Poly(allylamine)-Stabilized Colloidal Copper Nanoparticles: Synthesis, Morphology, and Their

Surface-Enhanced Raman Scattering Properties. *Langmuir* **2010**, *26*, 7469–7474.
28. Nam, C.; Kim, Y.-S.; Kim, W. B.; Cho, B. K. Magnetic Dipolar Interaction in NiFe Nanodot Arrays Formed on Vertical Carbon Nanotubes. *Nanotechnology* **2008**, *19*, 475703.
29. Nam, S. H.; Shim, H. −S.; Kim, Y. −S.; Dar, M. A.; Kim, J. G.; Kim, W. B. Ag or Au Nanoparticle-Embedded One-Dimensional Composite TiO_2 Nanofibers Prepared via Electrospinning for Use in Lithium-Ion Batteries. *ACS Appl. Mater. Interfaces* **2010**, *2*, 2046–2052.
30. Kim, Y. S.; Jang, H. S.; Kim, W. B. An Efficient Composite Hybrid Catalyst Fashioned from Pt Nanoparticles and Sb-Doped SnO_2 Nanowires for Alcohol Electro-Oxidation. *J. Mater. Chem.* **2010**, *20*, 7859–7836.
31. Armstrong, R. W.; Baschung, B.; Booth, D. W.; Samirant, M. Enhanced Propellant Combustion with Nanoparticles. *Nano Lett.* **2003**, *3*, 253–255.
32. Park, B.; Cho, K.; Yun, J.; Koo, Y. -S.; Lee, J. -H.; Kim, S. Electrical Characteristics of Floating-Gate Memory Devices with Titanium Nanoparticles Embedded in Gate Oxides. *J. Nanosci. Nanotechnol.* **2008**, *8*, 1–5.
33. Masuda, H.; Yamada, H.; Satoh, M.; Asoh, H.; Nakao, M.; Tamamura, T. Highly Ordered Nanochannel-Array Architecture in Anodic Alumina. *Appl. Phys. Lett.* **1997**, *71*, 2770–2772.
34. Masuda, H.; Fukuda, K. Ordered Metal Nanohole Arrays Made by a Two-Step Replication of Honeycomb Structures of Anodic Alumina. *Science* **1995**, *268*, 1466–1468.